ENCLOSURE

BYRON UNIT 1 REFUEL OUTAGE B1R05

RHR HEAT EXCHANGER NOZZLES

ULTRASONIC INDICATION SUMMARY

Prepared By:

G. Hagemann, CECo Byron SEC

1) BACKGROUND

Byron requested relief (Preservice Relief Request NR-13) from the NRC during Preservice Inspection for the volumetric examinations for the Residual Heat Removal Heat Exchanger (RHR) nozzle to vessel welds. The basis behind the request was due to the geometric restraints in performing the examination as a result of the configuration of the nozzle to vessel welds. The configuration of the nozzle is such that construction did not allow for relevant volumetric examination as the installation utilizes an internal reinforcing pad and a double bevel groove weld with a fillet reinforcement. The relief request was granted by the NRC and documented in their review of the Unit 1 Byron Preservice Inspection Program Docket # 50-455, SSER 7 Appendix K.

Byron requested similar relief for the Inservice Inspection program via submittal of Inservice Relief Request NR-12. This request for relief sought the same exemption for volumetric examinations of the nozzle to vessel welds and inner radius that had been granted during Preservice. This relief was granted for the inner radius inspection but requested that a "best effort" volumetric examination be performed on the nozzle to vessel welds. This is documented in the NRC Safety Evaluation of the Byron Units 1 and 2 First Ten Year Interval Inservice Inspection Program.

It should be noted that Braidwood had previously performed these examinations on their Unit 2 RHR Heat Exchangers in November of 1991 in response to their like Relief Request and identified the existence of numerous indications attributed to manufacturing defects. Braidwood solicited Westinghouse Corporation to perform a Fracture Mechanics Analysis in accordance with ASME Section XI IWB-3500 and/or IWB-3600. The analysis was initiated for both Byron and Braidwood Units 1 and 2 RHR Heat Exchangers Nozzles and subsequently, this methodology was accepted by the NRC for application at both Byron and Braidwood. This analysis (Westinghouse Report MMDT-SMT-062) accepted the existence of flaws up to and including 60% of the thickness of the material at the flaw location, extending 360° and surface connected. The analysis accepted these types of flaws for the entire 40 year service life of the vessel.

During Byron Unit 2 B2R03 Refueling Outage in spring of 1992, several similar indications were identified in all four nozzle to vessel welds for the 2A and 2B RHR Heat Exchangers. These welds were accepted by the Westinghouse Fracture Mechanics Analysis previously mentioned.

2) INTRODUCTION

Pursuant to the NRC response to Inservice Relief Request NR-12, a "best effort" ultrasonic examination was conducted on the Byron Unit 1 RHR Heat Exchanger nozzle to vessel welds.

During Byron Refueling Outage B1R05 the Unit 1 "B" RHR Heat Exchanger Outlet nozzle to vessel weld was scheduled for examination. Ultrasonic reflectors were identified in excess of 100% DAC (Distance Amplitude Correction) reference levels with definable depth. These indications were evaluated and determined to be in excess of the acceptance criteria defined in IWB-3500. The examination were expanded to include the "B" Inlet nozzle where similar indications in excess of IWB-3500 were recorded. Ultimately, all four Unit 1 RHR nozzle to vessel welds were examined and indications in excess of IWB-3500 were identified. These indications were sized and all were determined to be within the Westinghouse Fracture Mechanics Analysis performed for the Byron and Braidwood RHR Heat Exchangers and were determined to be acceptable for continued service.

These indications are consistent with the indications found at Braidwood and at Byron Unit 2 and are consistent with slag inclusions and/or lack of fusion in the fabrication process and are not service induced flaws.

As shown in this report all indications are within ASME Section XI Subarticle acceptance standards provided in IWB-3500 or IWB-3600. Those indications which were found to be acceptable analytically by the Fracture Mechanics Analysis will be monitored by examinations that will be conducted in future Byron Unit 1 Refueling Outage as required by ASME Section XI IWC-2420.

3) FABRICATION INFORMATION

The subject nozzles are on the tube side of the RHR Heat Exchangers. These heat exchangers were manufactured by Joseph Oats Corporation in 1975 in accordance with ASME Section III, NC-3200 Alternate Design Rules for Vessels. The heat exchanger vessel tube side is ASME Class 2 and the shell side is ASME Class 3. The nozzles are 3/8" nominal thickness (actual measured ultrasonic thickness is .400"), 13.875 inches outside diameter, SA-240 TP304 rolled plate welded to the 1 inch thick SA-240 TP304 rolled plate of the tube side vessel wall.

The weld configuration is a double bevel groove weld with an external 3/8" nominal fillet weld reinforcement. The welding process was performed using the shielded metal arc process with E308 electrodes. Joseph Oat personnel and their fabrication procedures indicate that the groove weld was backgouged at the root pass(es) during the welding process. The inside and outside surfaces of the welded joints were examined by the liquid penetrant method at the completion of welding. The welds were not radiographed during fabrication as due to the joint configuration. ASME Section III, 1974 Edition, NC-3352 does not require radiographic examination of angle joints between the shell and nozzle which exceed 30°. The ultrasonic examinations performed during this outage were the first volumetric examinations of these welds.

4) ULTRASONIC TECHNIQUES

The RHR heat exchanger nozzle to vessel welds were examined using a procedure that required a calibration which would produce an examination that meets the intent of ASME Section XI Appendix III requirements.

The examinations were conducted utilizing CECO NDE Procedure NDT-C-2 Revision 19. The examination was conducted utilizing an Ultrasonic Imaging Flaw Detector (P-Scan) which allows accurate interpretations of flaws and offers the advantage of consistent repeatability in the future.

Flaw indications were plotted on the P-Scan at the 50% DAC reference level and were sized to 50% of their maximum amplitude. Indications which exceed ASME Section XI IWB-3500 acceptance criteria will be monitored in future refueling outages as required by ASME Section XI, IWC-2420.

5) ULTRASONIC EXAMINATION RESULTS

Attachment A summarizes, for each nozzle, the recordable indications detected during ultrasonic examinations. The flaws were found not be surface connected, however following the methodology of ASME Section XI, IWA-3310(b), the flaws have been considered as surface flaws and are so noted on these tables. The a/t column values were established based on the nozzle wall thickness (.400").

6) EVALUATION OF ULTRASONIC EXAMINATION RESULTS

The Fracture Mechanics Analysis previously referenced in this report was performed by Westinghouse in accordance with the methodology and criteria provided in ASME Section XI IWB-3600. This evaluation developed maximum allowed flaw dimensions for normal operating conditions and emergency and faulted conditions. The results of the Fracture Mechanics Analysis has been used to develop an upper boundary flaw chart for the recorded indications. The complete Westinghouse analysis which developed this criteria is provided as Attachment B to this report. Figure 4-1 in the Westinghouse Analysis shows the developed chart.

All indications from Section 5 which were found to be in excess of the criteria in IWB-3500 have been found to be within the Fracture Mechanics Analysis allowable limits.

7) PRIMARY COOLANT WATER CHEMISTRY

The RHR heat exchanger tube side nozzles are exposed to only primary coolant water. The Chemistry requirements for primary coolant water are provided in Section 3/4.4.7 of the Byron Technical Specifications. These limits are 100 ppb dissolved oxygen when the temperature is greater than 250°F and 150 ppb for Fluoride and Chloride at all temperatures. A detailed discussion of Stress Corrosion-Cracking Susceptibility is provided in the Westinghouse Fracture Mechanics Evaluation MMDT-SMT-062 Section 3.4 which is provided as Attachment B to this report.

8) CONCLUSION

All the ultrasonic examination indications detected on the nozzle to vessel welds to the 1A and 1B RHR heat exchangers tube side nozzles have been found to be acceptable in accordance with ASME Section XI IWB-3500 or IWB-3600 as applicable. Therefore, with the prior NRC approval of the Byron/Braidwood evaluation methodology and guidance from NRC Generic Letter 91-18, system operability was not impacted.

Those flaws which have been determined to be acceptable by the Fracture Mechanics Analysis will be monitored in future Byron Unit 1 Refueling Outages as required by ASME Section XI IWC-2420.

The ultrasonic examination indications noted are consistent with those noted at Braidwood Unit 2 and at Byron Unit 2 and are consistent with fabrication flaws rather than service induced flaws.

These indications are acceptable for continued service without repair as defined in the Westinghouse Analysis.

ATTACHMENT A

INDICATION SUMMARY

Component: **1RH02AA** **Weld No:** **1RHXN-1 Outlet Nozzle**

A total of 17 indications above 50% DAC were recorded with 4 of these indications exceeding 100% DAC with definable length.

The following is a summary of indications which exceed 100% DAC and exhibit a definable depth and length as reported in Ebasco ultrasonic report number 93BY1-UT-028:

Ind.	Loc.	Max. Amp.	Lgth.	a**	a/l	a/t*
1	3.56-3.90"	100%	.34"	.095"	.28"	25%
2	4.00-4.36"	112%	.36"	.131"	.36"	35%
8	32.95-33.25"	200%	.30"	.170"	.56"	45%
9	34.37-34.60"	100%	.23"	.095"	.41"	25%

* a/t represents through wall percentages of indication utilizing the nozzle wall thickness (.400").

** Denotes ASME Section XI (Article IWA-3000) characterization (i.e. a=surface, 2a=subsurface).

Identified flaws were characterized as surface flaws per Table IWB 3514-2.

Component: **1RH02AA** **Weld No:** **1RHXN-2 Inlet Nozzle**

A total of 13 indications above 50% DAC were recorded with 5 of these indications exceeding 100% DAC with definable length.

The following is a summary of indications which exceed 100% DAC and exhibit a definable depth and length as reported in Ebasco ultrasonic report number 93BY1-UT-029:

Ind.	Loc.	Max. Amp.	Lgth.	a**	a/l	a/t*
1	.04-.36"	112%	.32"	.080"	.25"	21%
5	14.00-14.60"	100%	.60"	.095"	.16"	25%
8	28.60-29.00"	112%	.40"	.080"	.20"	21%
9	31.15-32.25"	158%	1.10"	.095"	.09"	25%
11	34.90-35.95"	158%	1.05"	.110"	.10"	30%

* a/t represents through wall percentages of indication utilizing the nozzle wall thickness (.400").

** Denotes ASME Section XI (Article IWA-3000) characterization (i.e. a=surface, 2a=subsurface).

Identified flaws were characterized as surface flaws per Table IWB 3514-2.

Component: **1RH02AB** **Weld No:** **1RHXN-1 Outlet Nozzle**

A total of 11 indications above 50% DAC were recorded with 2 of these indications exceeding 100% DAC with definable length.

The following is a summary of indications which exceed 100% DAC and exhibit a definable depth and length as reported in Ebasco ultrasonic report number 93BY1-UT-026:

Ind.	Loc.	Max. Amp.	Lgth.	a**	a/l	a/t*
1	3.84-4.20"	126%	.36"	.150"	.42"	40%
3	6.70-7.70"	126%	1.00"	.131"	.13"	35%

* a/t represents through wall percentages of indication utilizing the nozzle wall thickness (.400").

** Denotes ASME Section XI (Article IWA-3000) characterization (i.e. a=surface, 2a=subsurface).

Identified flaws were characterized as surface flaws per Table IWB 3514-2.

Component: **1RH02AB** **Weld No:** **1RHXN-2 Inlet Nozzle**

A total of 21 indications above 50% DAC were recorded with 11 of these indications exceeding 100% DAC with definable length.

The following is a summary of indications which exceed 100% DAC and exhibit a definable depth and length as reported in Ebasco ultrasonic report number 93BY1-UT-027:

Ind.	Loc.	Max. Amp.	Lgth.	a**	a/l	a/t*
3	5.48-6.20"	112%	.87"	.080"	.09"	21%
6	16.85-17.20"	100%	.35"	.080"	.35"	21%
8	25.95-27.15"	158%	1.20"	.150"	.12"	40%
9	31.65-32.00"	200%	.35"	.080"	.23"	21%
10	31.50-31.95"	158%	.45"	.080"	.17"	21%
11	30.65-31.00"	100%	.35"	.080"	.23"	21%
15	36.25-36.57"	100%	.32"	.060"	.19"	16%
16	36.50-36.75"	112%	.25"	.080"	.32"	21%
17	37.20-39.00"	126%	1.80"	.080"	.04"	21%
18	37.61-37.93"	200%	.32"	.080"	.25"	21%
19	37.10-38.00"	126%	.90"	.080"	.09"	21%

* a/t represents through wall percentages of indication utilizing the nozzle wall thickness (.400").

** Denotes ASME Section XI (Article IWA-3000) characterization (i.e. a=surface, 2a=subsurface).

Identified flaws were characterized as surface flaws per Table IWB 3514-2.

ATTACHMENT B

FRACTURE MECHANICS ANALYSIS

MMDT-SMT-062(92)

FRACTURE MECHANICS EVALUATION
BYRON AND BRAIDWOOD UNITS 1 AND 2 RESIDUAL HEAT EXCHANGER TUBE SIDE INLET AND OUTLET NOZZLES

March 1992

W. H. Bamford
H. Jambusaria
Y. S. Lee

WESTINGHOUSE ELECTRIC CORPORATION
Nuclear and Advanced Technology Division
P.O. Box 2728
Pittsburgh, Pennsylvania 15230-2728

TABLE OF CONTENTS

SECTION 1.0
INTRODUCTION

This fracture mechanics evaluation has been carried out to determine the largest size of indications which can be accepted according to the rules of Section XI, paragraph IWB 3600 for the residual heat exchanger inlet and outlet nozzles. The results of this evaluation are presented in flaw evaluation charts in Section 4, and the technical basis for construction of the charts is contained in the remaining sections.

1.1 Code Acceptance Criteria

The evaluation procedures and acceptance criteria for indications in austenitic stainless piping are contained in paragraph IWB 3640 of ASME Section XI.[1] The evaluation procedure is applicable to all the materials within a specified distance from the weld centerline, $\sqrt{rt}$, where r = the pipe nominal outside radius and t is the nominal wall thickness. For example, at the RHX nozzle, this distance is calculated to be 1.62 inches, which encompasses regions of the heat exchanger, as well as part of the RHR line. All the materials in this region are Type 304 stainless steel.

The evaluation process begins with a flaw growth analysis, with the requirement to consider growth due to both fatigue and stress corrosion cracking. For pressurized water reactors only fatigue crack growth need be considered, as discussed in section 3. The methodology for the fatigue crack growth analysis is described in detail in section 3.

The calculated maximum flaw dimensions at the end of the evaluation period are then compared with the maximum allowable flaw dimensions for both normal operating conditions and emergency and faulted conditions, to determine acceptability for continued service. Provisions are made for considering flaws projected both circumferentially and axially.

In IWB 3640 the allowable flaw sizes have been defined in the tables based on maintaining specified safety margins on the loads at failure. These margins are 2.77 for normal and upset conditions and 1.39 for emergency and faulted

conditions. The calculated failure loads are different for the base metal and the flux welds, which have different fracture toughness values, as discussed in section 2. The failure loads, and consequently the allowable flaw sizes, are larger for the base metal than for the welds. Allowable flaw sizes for welds are contained in separate tables, in IWB 3640.

1.2 Geometry

The geometry of the residual heat exchanger is shown in Figure 1-1, with the details of the inlet and outlet nozzles of the tube side shown in Figure 1-2. The notation used for surface flaws in this work is illustrated in figure 1-3.

The fracture and fatigue crack growth evaluations carried out to develop the handbook charts have employed the recommended procedures and material properties for stainless steel as prescribed in paragraph IWB 3640 and Appendix C of Section XI.

TOP VIEW

SIDE VIEW

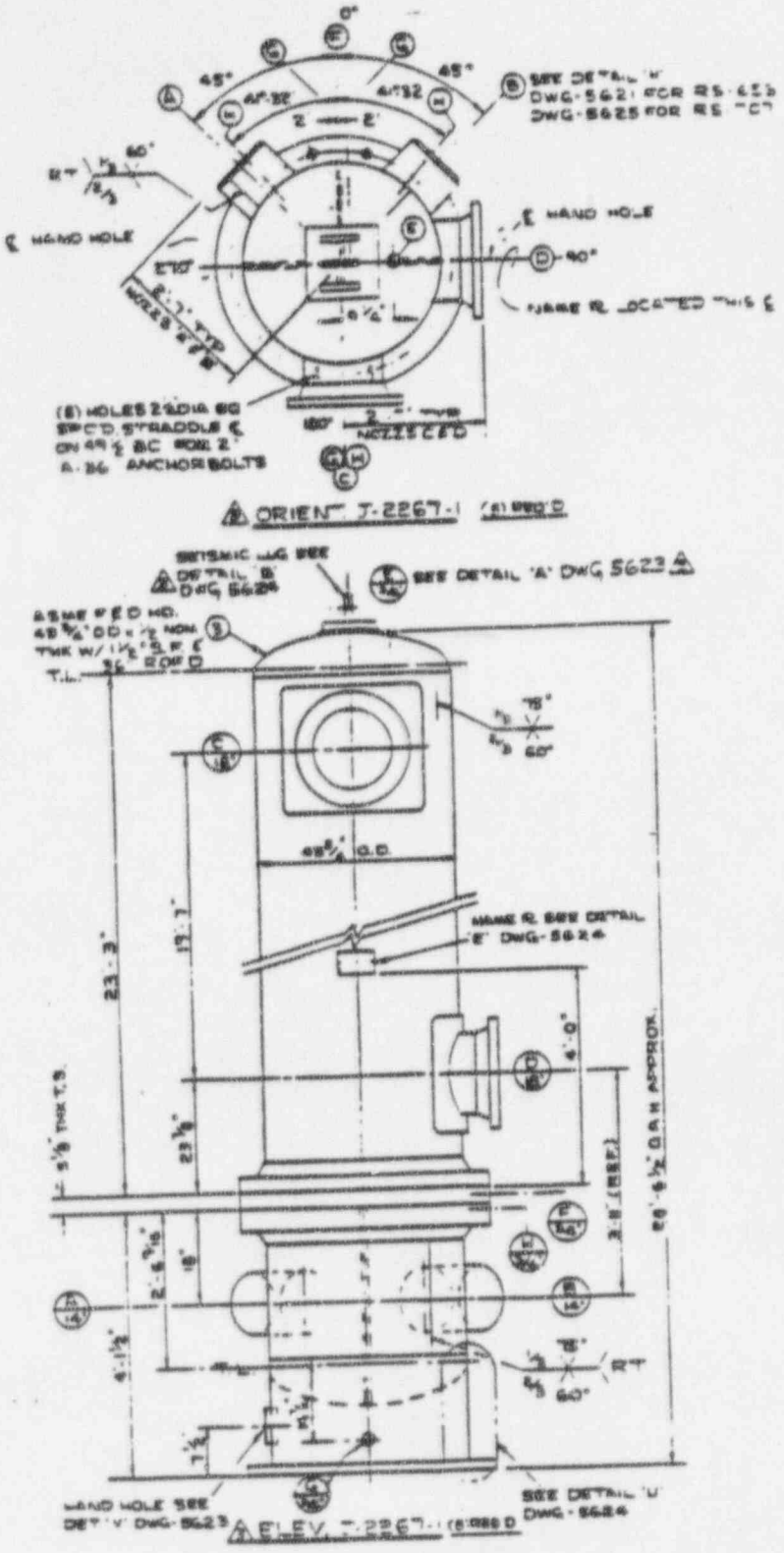

Figure 1-1. Geometry of the Residual Heat Exchanger

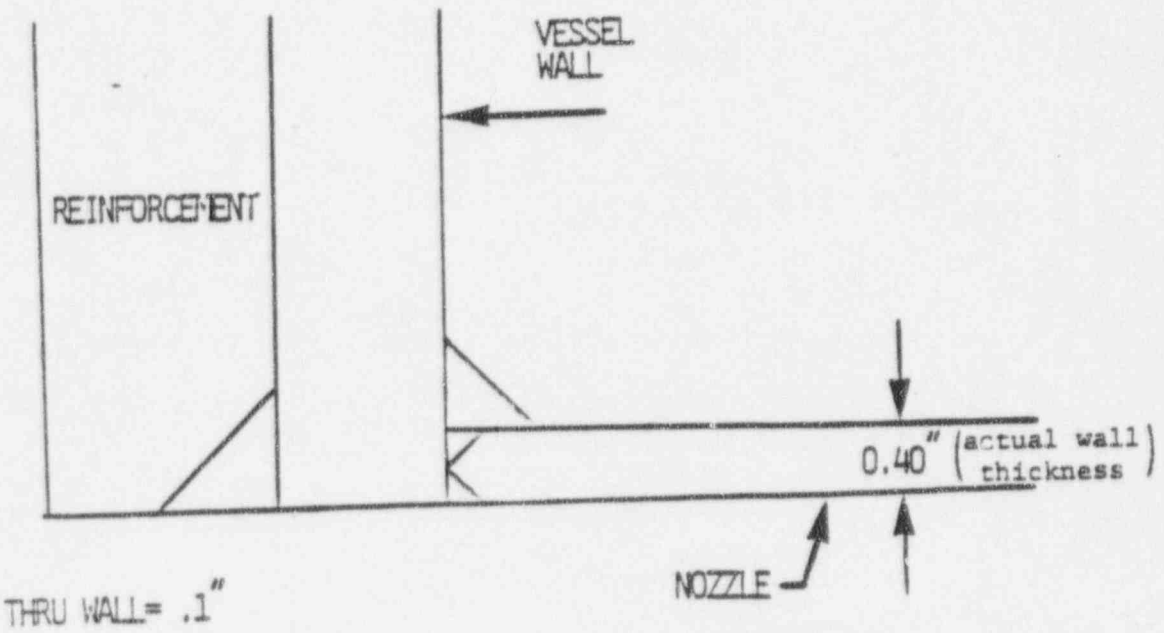

Figure 1-2. Geome[illegible] Tube Side Nozzles
(Inlet and Out[illegible] are Identical)

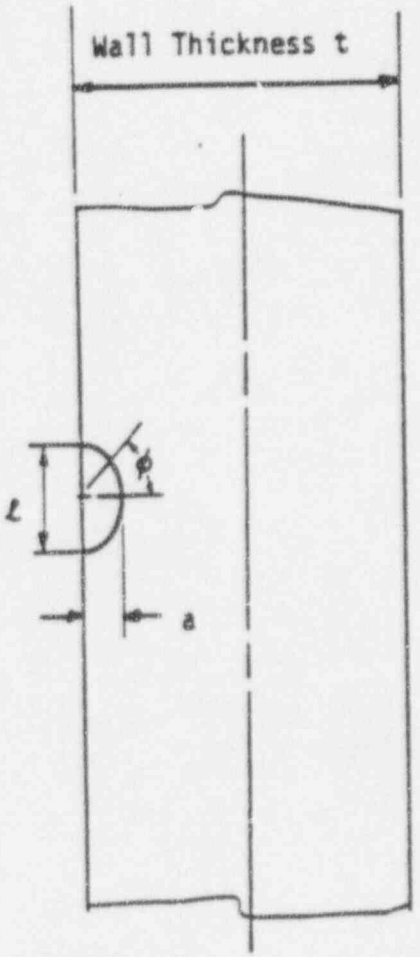

Figure 1-3. Typical Notation for Surface Flaw Indications

SECTION 2.0
LOAD CONDITIONS, FRACTURE ANALYSIS METHODS AND MATERIAL PROPERTIES

The loading conditions used in the analyses described herein were taken directly from the equipment specification. The fracture analysis methods are the most advanced which are now available, and the material properties are the latest available properties contained in the ASME Code.

2.1 Transients and Load Conditions

The design transients for the residual heat exchanger are very minimal, because this component operates only during plant shutdown conditions. Therefore the only transient conditions which it experiences are the startup and shutdown of the system, which coincides with the shutdown and startup of the plant, respectively. The appropriate limiting load conditions for the location of interest are discussed next.

The loading conditions which were evaluated include thermal expansion (normal and upset), pressure, deadweight and seismic (OBE and SSE) loadings. The RHR piping forces and moments for each condition were obtained from the ASME Code Section III calculations previously performed by Sargent and Lundy and Westinghouse for Byron and Braidwood Units 1 and 2 [2-5]. These loads [6] were compared with the Equipment Specification design loadings for the heat exchanger nozzles (G-679150 Rev. 1) and found to be bounded by them. As a consequence of this comparison, the evaluation performed using the design loadings, is applicable to Byron and Braidwood Units 1 and 2. Residual stresses were not used in this portion of the evaluation, in compliance with the Code guidelines. A further discussion of residual stresses is contained in Section 3.2. The stress intensity values were calculated using the following equations:

$$SI = P_m + P_b$$

$$SI = \frac{F_x}{A} + \frac{1}{Z}\left[M_x^2 + M_y^2 + M_z^2\right.$$

where

F_x = axial force component (membrane)

M_x, M_y, M_z = moment components (bending)

A = cross-section area

Z = section modulus

The section properties A and Z at the weld location were determined based on the minimum pipe dimensions. This is conservative since the measured wall thickness at the weld is generally larger.

The following load combinations were used.

A. Normal/Upset - Primary Stress

Pressure + Deadweight + OBE

B. Emergency/Faulted - Primary Stress

Pressure + Deadweight + SSE

C. Normal/Upset - Total Stress

Pressure + Deadweight + OBE + Normal Thermal

D. Emergency/Faulted - Total Stress

Pressure + Deadweight + SSE + Normal Thermal

2.2 Stress Intensity Factor Calculations

One of the key elements of the fatigue crack growth calculations is the determination of the driving force or stress intensity factor (K_I). This was done using expressions available from the literature. In all cases the stress intensity factor calculations utilized a representation of the actual stress profile rather than a linearization. This was necessary to provide the most

accurate determination possible. The stress profile was represented by a cubic polynomial:

$$\sigma(x) = A_0 + A_1 \frac{x}{t} + A_2 \left(\frac{x}{t}\right)^2 + A_3 \left(\frac{x}{t}\right)^3 \qquad (2\text{-}1)$$

where
- x = is the coordinate distance into the wall
- t = wall thickness
- σ = stress perpendicular to the plane of the crack
- A_i = coefficients of the cubic fit

For the surface flaw with length six times its depth, the stress intensity factor expression of [McGowan and Raymund [7]][a,c,e] was used. The stress intensity factor $K_I(\phi)$ can be calculated anywhere along the crack front. The point of maximum crack depth is represented by $\phi = 0$. The following expression is used for calculating $K_I(\phi)$, where d is the angular location around the crack.

$$K_I(\phi) = \left[\frac{\pi a}{Q}\right]^{0.5} (\cos^2\phi + \frac{a^2}{c^2}\sin^2\phi)^{1/4} (A_0 H_0 + \frac{2}{\pi}\frac{a}{t}A_1 H_1 + \frac{1}{2}\frac{a^2}{t^2}A_2 H_2 + \frac{4}{3\pi}\frac{a^3}{t^3}A_3 H_3) \qquad (2\text{-}2)$$

The magnification factors $H_0(\phi)$, $H_1(\phi)$, $H_2(\phi)$ and $H_3(\phi)$ are obtained by the procedure outlined in reference [8].

The stress intensity factor calculation for a semi-circular surface flaw, (aspect ratio 2:1) was carried out using the expressions developed by [Raju and Newman [8]][a,c,e]. Their expression utilizes the same cubic representation of the stress profile and gives the same result as the expression of [McGowan and Raymund][a,c,e] for the 2:1 aspect ratio flaw, and the form of the equation is similar to that of [McGowan and Raymund][a,c,e] above.

The stress intensity factor expression used for a continuous surface flaw was that developed by [Buchalet and Bamford [9]]^{a,c,e}. Again the stress profile is represented as a cubic polynomial, as shown above, and these coefficients as well as the magnification factors are combined in the expression for K_I

$$K_I = \sqrt{\pi a}\left[A_0F_1 + \frac{2a}{\pi}A_1F_2 + \frac{a^2}{2}A_2F_3 + \frac{4}{3\pi}a^3A_3F_4\right]^{a,c,e} \qquad (2\text{-}3)$$

where F_1, F_2, F_3, F_4 are magnification factors, available in [9].

2.3 Fracture Toughness

The residual heat exchanger is stainless steel type 304. The weld at the nozzle was made by the shielded metal arc process, as verified by the shop traveller, and the weld procedure referenced therein.

The fracture toughness of the base metal has been found to be very high, even at operating temperatures [10], where the J_{Ic} values have been found to be well over 2000 in-lb/in^2. Fracture toughness values for weld materials have been found to display much more scatter, with the lowest reported values significantly lower than the base metal toughness. Although the J_{Ic} values reported have been lower, the slope of the J-R-curve is still large for these J_{Ic} cases. Representative values for J_{Ic} were obtained from the results of Landes, et. al. [11], where the following values were obtained, and used in the development of the fracture evaluation methods:

[for shielded metal arc welds: J_{Ic} = 990 in lb/in^2.]^{a,c,e}

2.4 THERMAL AGING

Thermal aging at operating temperatures of reactor primary piping can reduce the fracture toughness of cast stainless steels and, to a lesser degree, stainless steel weldments. Because of the lower operating temperature (400°F) of the residual heat exchanger, and the fact that the materials are type 304 stainless (not cast), thermal aging in this component will be negligible.

2.5 Allowable Flaw Size Determination

The critical flaw size is not directly calculated as part of the flaw evaluation process for stainless steels. Instead, the failure mode and critical flaw size are incorporated directly into the flaw evaluation technical basis, and therefore into the tables of "Allowable End-of-Evaluation Period Flaw Depth to Thickness Ratio," which are contained in paragraph IWB 3640.

Rapid, nonductile failure is possible for ferritic materials at low temperatures, but is not applicable to stainless steels. In stainless steel materials, the higher ductility leads to two possible modes of failure, plastic collapse or unstable ductile tearing. The second mechanism can occur when the applied J integral exceeds the J_{Ic} fracture toughness, and some stable tearing occurs prior to failure. If this mode of failure is dominant, the load carrying capacity is less than that predicted by the plastic collapse mechanism.

The allowable flaw sizes of paragraph IWB 3640 for the high toughness base materials were determined based on the assumption that plastic collapse would be achieved and would be the dominant mode of failure. [However, due to the reduced toughness of the shielded metal arc welds, it is possible that crack extension and unstable ductile tearing could occur and be the dominant mode of failure. This consideration in effect reduces the allowable end of interval flaw sizes for flux welds relative to the austenitic wrought type 304 vessel and piping materials, and has been incorporated directly into the evaluation tables.]^{a,c,e}

SECTION 3.0
FATIGUE CRACK GROWTH

In applying Code acceptance criteria as introduced in section 1, the final flaw size a_f is defined as the flaw size to which the detected flaw is calculated to grow at the end of a specified period, or until the next inspection time. This section will examine each of the calculations, and provide the methodology used as well as the assumptions.

3.1 Analysis Methodology

The methods used in the crack growth analysis reported here are the same as those suggested by Section XI of the ASME Code. The analysis procedure involves postulating an initial flaw at specific regions and predicting the growth of that flaw due to an imposed series of loading transients. The input required for a fatigue crack growth analysis is basically the information necessary to calculate the parameter ΔK_I which depends on crack and structure geometry and the range of applied stresses in the area where the crack exists. Once ΔK_I is calculated, the growth due to that particular stress cycle can be calculated by equations given in section 2.2 and figure 3-1. This increment of growth is then added to the original crack size, and the analysis proceeds to the next transient. The procedure is continued in this manner until all the transients known to occur in the period of evaluation have been analyzed.

The only transients considered in the analysis were the startup and shutdown of the RHR system. These transients are spread equally over the design lifetime of the vessel.

Crack growth calculations were carried out for a range of flaw depths, and three basic types. The first two were surface flaws, one with length equal to six times the depth and another with length equal twice the depth. Third was a continuous surface flaw, which represents a worst case for surface flaws.

3.2 Crack Growth Rate Reference Curves

The reference crack growth law used for the stainless steel was taken from that developed by the Metal Properties Council - Pressure Vessel Research Committee Task Force in Crack Propagation Technology. The reference curve has the equation:

$$\frac{da}{dN} = CFS\,\Delta K^n \qquad (3\text{-}7)$$

where $\frac{da}{dN}$ = crack growth rate, inches per cycle

C = material coefficient ($C = 2.0 \times 10^{-19}$)
F = frequency coefficient for loadings ($F = 2.0$)
S = R ratio correction coefficient ($S = 1.0 - 0.502\,R^2)^{-4.0}$
n = material property slope ($=3.0321$)
ΔK = stress intensity factor range, psi $\sqrt{in}$

This equation appears in Section XI, Appendix C (1989 Addendum) for air environments and its basis is provided in reference [12], and shown in figure 3-1. For water environments, an environmental factor of 2 was used, based on the crack growth tests in PWR environments reported by Bamford [13].

3.3 Residual Stresses

Since the residual heat exchanger vessel-to-piping welds were not stress-relieved, residual stresses are clearly present. For fatigue crack growth analyses, these stresses were included directly.

In general the distribution of res[illegible]tresses is strongly dependent on the degree of constraint of the struct[illegible]e stiffer the structure the higher the residual stresses. For a thi[illegible]arge diameter pipe the residual stresses will be lower than a sma[illegible]r thick-walled pipe. This has been found by a number of investigator[illegible]e is general agreement that the distribution of residual stresses[illegible]e near the surface, and then

compressive near the center of the wall after which it reverses to become tensile at the outer surface.

The residual stresses were taken from work reported by General Electric [14] and E. Rybicki [15], which included both measurements of residual stress and finite element calculations. Both approaches were found to be in agreement, and included a range of pipe sizes from 4 inches to 28 inches in diameter. The stresses were found to peak at the weld, as shown in Figure 3-2 for a 10 inch diameter pipe. the through wall distribution of residual stresses used in this analysis was taken from the work of Rybicki, and is shown in Figure 3-3. This distribution is for a 10 inch schedule 160 pipe with a thickness of 1.125 inches, which is a much stiffer configuration than the 14 inch diameter, 0.375 inch thick junction at the heat exchanger nozzle.

3.4 Stress Corrosion Cracking Susceptibility

In evaluating flaws, all mechanisms of subcritical crack growth must be evaluated to ensure that proper safety margins are maintained during service. Stress corrosion cracking has been observed to occur in stainless steel in operating BWR piping systems. The discussion presented here is the technical basis for not considering this mechanism in the present analysis. The residual heat exchanger tube side nozzles are exposed to only primary coolant water.

For all Westinghouse plants, there is no history of cracking failure in the reactor coolant system loop piping. For stress corrosion cracking (SCC) to occur in piping. the following three conditions must exist simultaneously: high tensile stresses, a susceptible material, and a corrosive environment. Since some residual stresses and some degree of material susceptibility exist in any stainless steel piping, the potential for stress corrosion is minimized by proper selection of a material immune to SCC as well as preventing the occurrence of a corrosive environment. The material specifications consider compatibility with the system's operating environment (both internal and external) as well as other materials in the system, applicable ASME Code rules, fracture toughness, welding, fabrication, and processing.

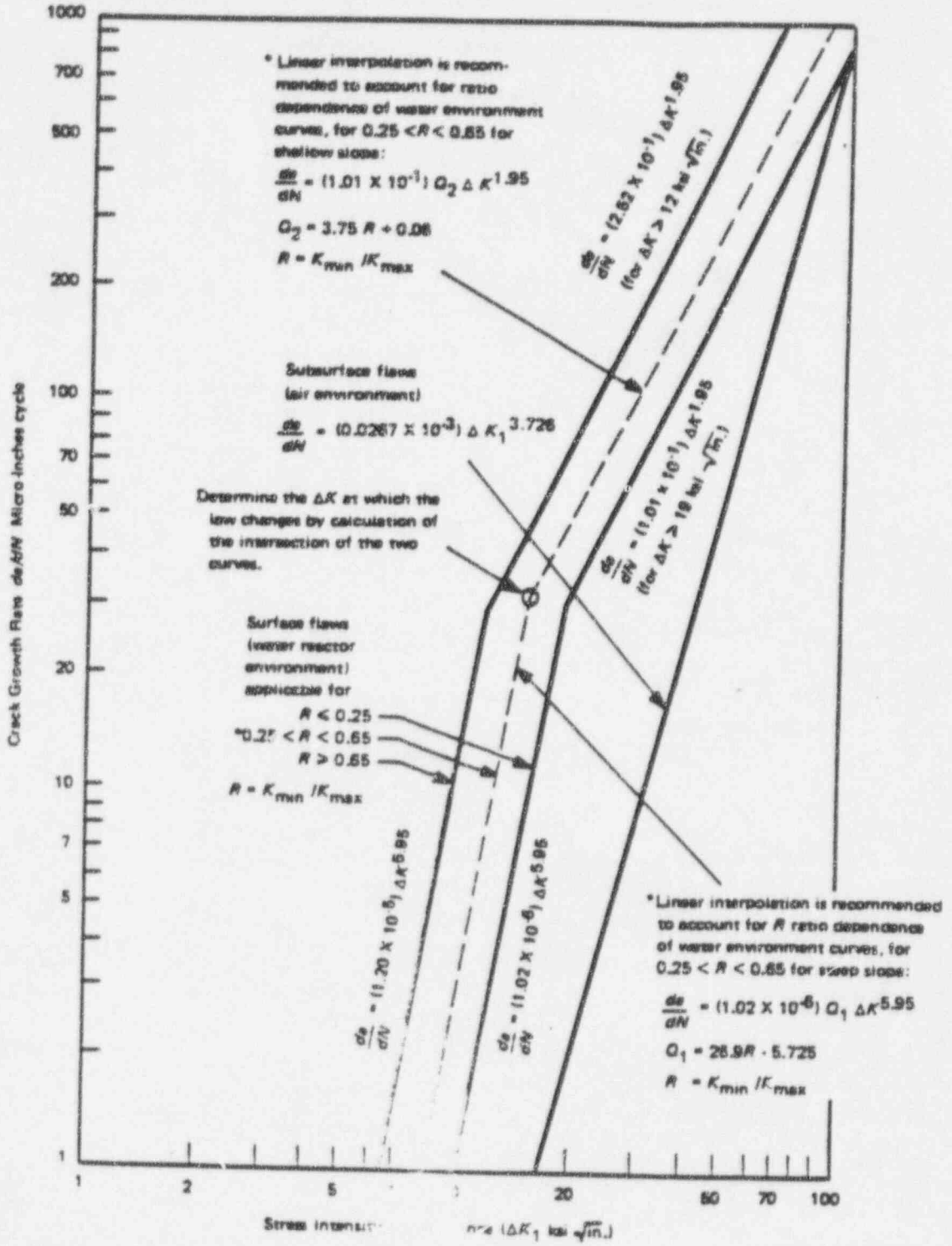

Figure 3-1. Reference Crack Gro[illegible]urves for Stainless Steel in Air Environments [12].

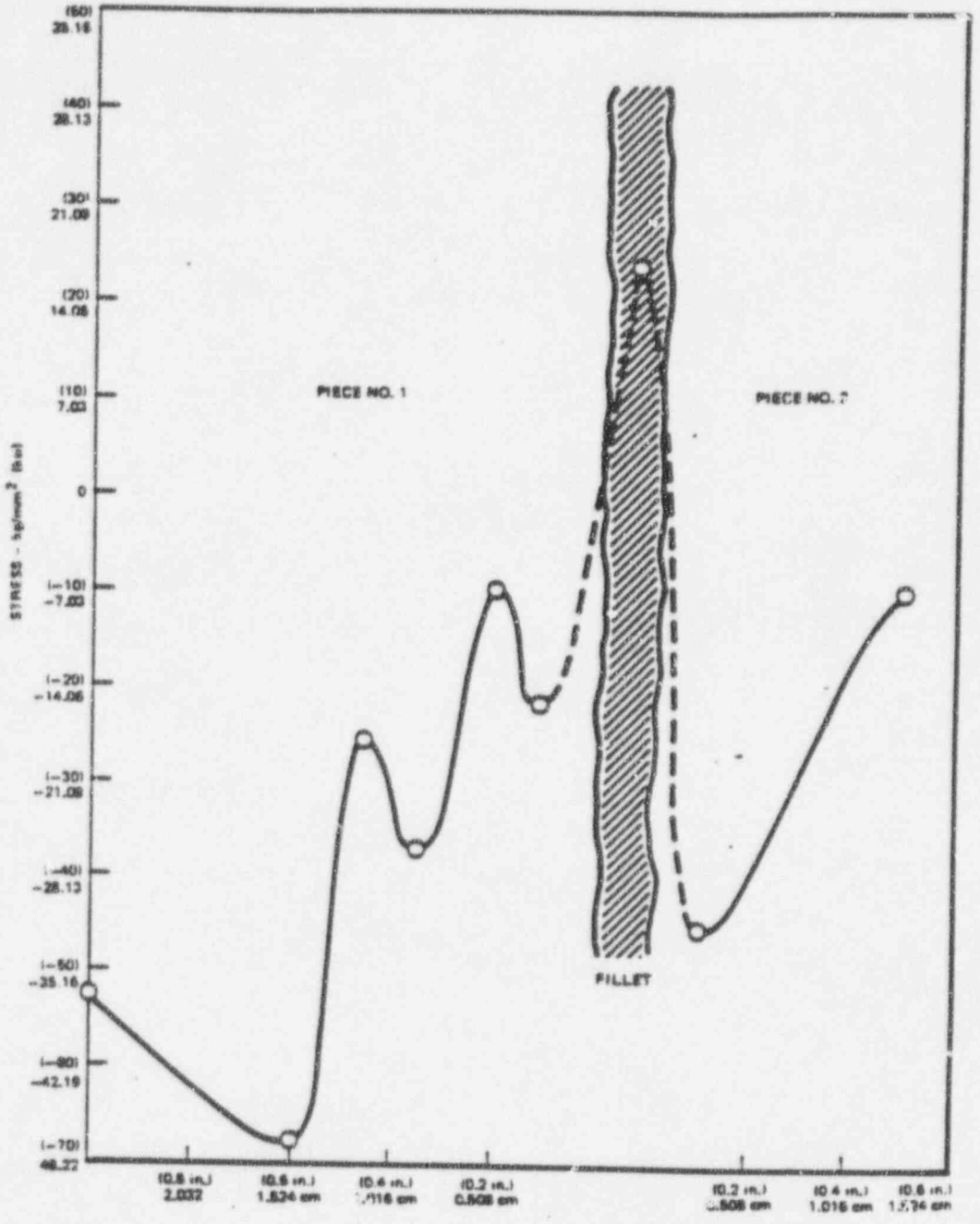

Figure 3-2. Maximum Principal Surface Residual Stress for a 10 inch Schedule 160 Pipe [14]

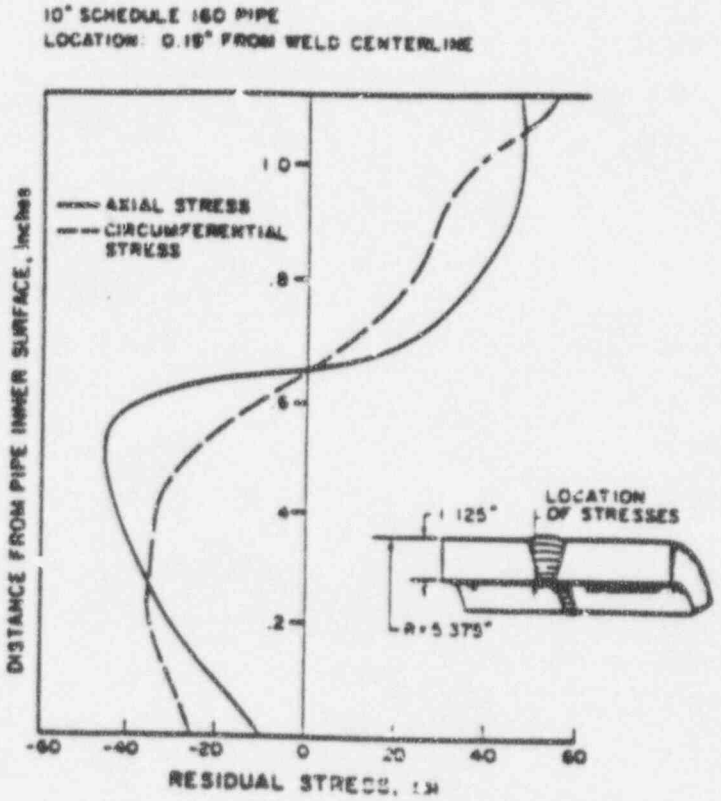

Figure 3-3. Through Wall Distributio[n] [o]f Residual Stress in a 10 Inch, Schedule 160 Pipe, in a Cross Section [a]t the Weld Center Line [15]

WPF1260J/032792:10

SECTION 4.0

4.1 Flaw Evaluation Charts Construction

The acceptance criteria for surface flaws have been presented in Section 1. For flaw evaluation in stainless steels, only the fatigue crack growth results must be calculated. The allowable flaw depths were determined directly from the tables in IWB 3640.

The first set of data required for surface flaw chart construction is the final flaw size a_f. As defined in IWB-3611 of ASME Code Section XI, a_f is the flaw depth resulting from growth during a specific time period, which can be the next scheduled inspection of the component, or until the end of design lifetime. Therefore, the final depth, a_f after a specific service period of time must be used as the basis for evaluation.

The final flaw size a_f can be calculated by fatigue crack growth analysis, which has been performed covering a range of postulated flaw sizes, and flaw shapes. The crack growth calculational methods have been discussed in Section 3. The results of the crack growth calculation showed that growth for a complete range of crack sizes, up to 60 percent of the wall thickness was inconsequential for the entire service life of 40 years. This was expected, since the region sees so few cycles.

The allowable flaw size for stainless steel is obtained directly from tables in paragraph IWB 3640, so the evaluation process is very straight forward. The allowable flaw size is calculated based on the most limiting transient for all normal operating conditions. Similarly, the allowable flaw size for emergency and faulted conditions is determined. The theory and methodology for the calculation of the allowable flaw sizes have been provided in Section 2 and Reference 16. Allowable flaw sizes were calculated for a range of flaw shapes.

The two basic dimensionless parameters, which can fully address the characteristics of surface flaw, have been used for the evaluation chart construction. Namely,

- o Flaw Length divided by the circumference, ℓ/c
- o Flaw Depth parameter a/t

where,

- t = wall thickness, in.
- a = flaw depth, in.
- ℓ = flaw length, in.
- c = pipe circumference, in.

The flaw evaluation chart for the residual heat exchanger inlet and outlet nozzles is shown in Figure 4-1. The chart has the following characteristics:

- o The flaw length/circumference ℓ/c was plotted as the abscissa from 0 to .5. For values of ℓ/c which exceed 0.5, use the results for ℓ/c = 0.5.

- o The flaw depth parameter a/t was plotted as the ordinate.

- o The upper boundary curve shows the maximum acceptable flaw depth based on flaw evaluation, beyond which no surface flaw is acceptable for continued service without repair. This upper bound curve has been determined by the fracture and fatigue evaluations described herein. using Tables IWB 3641-5 and IWB 3641-6, for shielded metal arc welds.

- o Any surface indication which falls below the boundary curve will be acceptable by the code rules, based on the analytical justification provided herein. However, IWB-2420 of ASME Section XI requires future monitoring of such indications.

A detailed example on the use of the curves for a surface flaw is presented below:

Surface Flaw Example

Now suppose an indication is to be evaluated using the charts. For the circumferential orientation:

$a = 0.10"$ $\quad \ell = 6.1"$
$t = 0.40"$ $\quad c = 44.0"$

The flaw characterization parameters then become:

$a/t = 0.250$
$\ell/c = 0.139$

Plotting these parameters on the surface flaw evaluation chart of Figure 4-1, it is quickly seen that the indication is acceptable.

4.2 Conservatisms in the Flaw Evaluation

The stress and fracture analysis results presented herein have been structured to be conservative at each step, to ensure that the final result will be conservative.

The stresses applied to the heat exchanger nozzles were taken from the vessel equipment specification loads, which represent bounding loads for the structure. The actual loads for the Byron and Braidwood Units 1 and 2 heat exchangers [6] are about 60 percent of the design loads.

The residual stresses used in the analysis were taken from a combination of measurements and analysis for a 10 inch schedule 160 pipe. The smaller pipe diameter and larger thickness (1.125 inches) for this pipe mean that the residual stress distribution used here will be very conservative relative to the heat exchanger nozzle.

Since the publication of the flaw evaluation criteria and methodology for stainless steel [16] a number of experiments have been carried out on large fracture toughness specimens and full size pipes with both submerged arc welds

and shielded metal arc welds [17]. These experiments have shown that the fracture toughness from these larger specimens is higher than the toughness values used in the development of the flaw evaluation methods. Therefore the flaw evaluation results presented here are conservative.

A further conservatism is added to this fracture evaluation by using the fracture criteria for a class 1 piping system for a class 2 component. There are presently no flaw evaluation criteria for class 2 components, but presumably if they were to be developed, smaller margins could be justified, with resulting larger allowable flaw sizes.

The indication depths from the inspections have been compared with the thickness of the pipe, with no benefit taken of the additional thickness resulting from the large fillet weld on the outside surface of the nozzle. As shown in Figure 1-2, this fillet weld is immediately above the indications, and so the actual percentage flaw penetration is smaller than that reported.

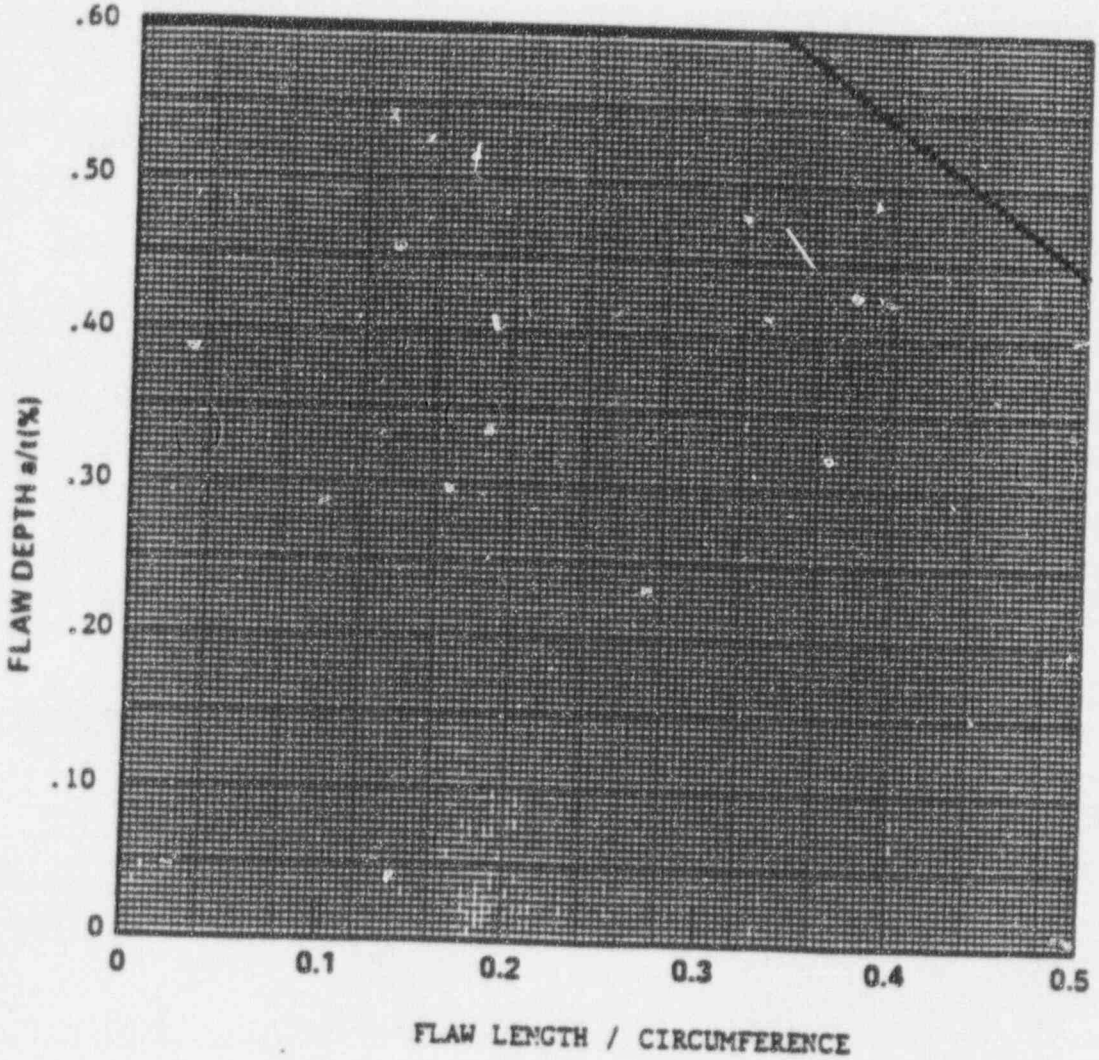

Figure 4-1 Flaw Evaluation Chart for Byron and Braidwood Units 1 and 2 Residual Heat Exchanger Tube Side Nozzles

SECTION 5.0
REFERENCES

1. ASME Code Section XI, "Rules for Inservice Inspection of Nuclear Power Plant Components," 1983 edition (used for updated code allowable limits); 1983 edition, Winter 1985 Addendum (used for flaw evaluation of austenitic stainless steel piping); 1989 edition (used for reference crack growth curve, stainless steel).

2. Jambusaria, H., "Residual Heat Exchangers: Braidwood Unit 2," Westinghouse Report No. 031804 Rev. 0, Jan. 24, 1986.

3. Jambusaria, H., "Residual Heat Exchangers: Byron Unit 1," Westinghouse Report No. 031805 Rev. 0, 2/27/92.

4. Jambusaria, H., "Residual Heat Exchangers: Byron Unit 2," Westinghouse Report No. 031806 Rev. 0, 2/27/92.

5. Jambusaria, H., "Residual Heat Exchangers: Braidwood Unit 1," Westinghouse Report No. 031803 Rev. 0, 2/27/92.

6. Letter #BPM #1577 from D. J. Skoza of Commonwealth Edison Company to Janet Bunecicky of Westinghouse Electric Corporation, Subject: RHR Heat Exchanger Nozzle Loads, dated 2/12/92.

7. McGowan, J. J. and Raymund, M., "Stress Intensity Factor Solutions for Internal Longitudinal Semi-elliptic Surface Flaw in a Cylinder Under Arbitrary Loading", ASTM STP 677, 1979, pp. 365-380.

8. Newman, J. C. Jr. and Raju, I. S., "Stress Intensity Factors for Internal Surface Cracks in Cylindrical Pressure Vessels", ASME Trans., Journal of Pressure Vessel Technology, Vol. 102, 1980, pp. 342-346.

9. Buchalet, C. B. and Bamford, W. H., "Stress Intensity Factor Solutions for Continuous Surface Flaws in Reactor Pressure Vessels", in Mechanics of Crack Growth, ASTM, STP 590, 1976, pp. 385-402.

10. Bamford, W. H. and Bush, A. J., "Fracture of Stainless Steel," in Elastic Plastic Fracture, ASTM STP 668, 1979.

11. Landes, J. D., and Norris, D. M., "Fracture Toughness of Stainless Steel Piping Weldments," presented at ASME Pressure Vessel Conference, 1984.

12. James, L. A., and Jones, D. P., "Fatigue Crack growth Correlations for Austenitic Stainless Steel in Air," in Predictive Capabilities in Environmentally Assisted Cracking," ASME publication PVP-99, Dec. 1985.

13. Bamford, W. H., "Fatigue Crack Growth of Stainless Steel Piping in a Pressurized Water Reactor Environment," Trans ASME, Journal of Pressure Vessel technology, Feb. 1979.

14. "Studies on AISI Types 304, 304L, and 347 Stainless Steels for BWR Application, April-June 1975," General Electric Report NEDO-20985-1, September 1975.

15. Rybicki, E. F., McGuire, P. A., Merrick, E., and West, J., "The Effect of Pipe Wall Thickness on Residual Stresses Due to Girth Welds," Trans ASME, Journal of Pressure Vessel Technology, Vol 104, August 1982.

16. "Evaluation of Flaws in Austenitic Steel Piping," Trans ASME, Journal of Pressure Vessel Technology, Vol. 108, Aug. 1986, pp. 352-366.

17. Wilkowski, G. et. al., "Analysis of Experiments on Stainless Steel Flux Welds," Battelle Columbus labs report for USNRC, number NUREG/CR 4878, April 1987.